Journal of Ceramic Processing Research. Vol. 11, No. 1, pp. 20~24 (2010)

J O U R N A L O F
Ceramic Processing Research

Effect of a colloidal SiO_2 coating to crack healing and the bending strength of Si_3N_4 ceramics

K.W. Nam[a,*] and J. S. Kim[b]
[a]*Pukyong National University, Busan 608-739, Korea*
[b]*NGETech Inc., 1545-5 Songjeong, Gangseo, Busan 618-818, Korea*

This is study analyzed the surface morphology of Si_3N_4 composite ceramics as functions of the heat-treatment temperature and the additive SiO_2. The additive colloidal SiO_2 and a coating of the colloidal SiO_2 on cracks was found to significantly increase the bending strength. Moreover, the presence of the additive TiO_2 resulted in decreasing the crack healing temperature by 300 K. Meanwhile, the bending strength of a specimen with the additive colloidal SiO_2 was revealed to be higher than that without colloidal. In addition, the bending strength of a specimen coated with colloidal SiO_2 was found to be much higher that of a non-coated specimen. During an in-situ observation, a fog-like phenomenon appeared on the surface of the crack-healed specimen at 1,573 K. When using an SPM (Scanning Probe Microscope), both of the crack-healed specimens, i.e. the one coated and non-coated with the colloidal SiO_2, were found to have completely healed at 1,273 K. However, cracks existed in both cases at 1,573 K. This can be regarded as the result of the evaporation of the SiO_2 at high temperatures. Crystallized $Y_2Si_2O_7$, $Y_2Ti_2O_7$ and SiO_2 were employed as the crack-healing materials of Si_3N_4 composite ceramics. A large amount of Si and O, and a minute amount of C were detected using an EPMA (Electron Probe X-Ray Micro Analyzer). The heat treatment temperature was found to result in an increase in Si and O and a concurrent decrease in C. Higher levels of Si and O were detected on the specimens with the SiO_2 additive than in ones when the additive SiO_2 was not present. Meanwhile, significantly higher levels of O were detected in the specimen coated with the colloidal SiO_2.

Key words: Si_3N_4 ceramics, SiO_2 colloidal coating, Hybride binder, In-situ observation, Crack-healing, Morphology.

Introduction

Some engineering ceramics such as silicon nitride (Si_3N_4) have been known to have crack-healing properties [1-8]. Many advantages can be obtained by applying these crack-healing properties to structural members present in engineering designs. These advantages include: 1) an increase in the reliability of the structural ceramic components; 2) a decrease in the processing costs of ceramics; and 3) a decrease in the maintenance expenses and concurrent extension of the lifecycle. The crack-healing properties of ceramics are known to originate from the SiO_2 oxides formed when these ceramics are heat treated at the atmospheric level [8-11]. Authors have evaluated the crack-healing properties of Al_2O_3 [12, 13], Si_3N_4 [14-18] and SiC [11, 19] ceramics. In addition, authors have also analyzed the improvement in bending strength brought about by synthesizing SiO_2 powder and colloidal SiO_2 during the sintering of the ceramics [15, 16]. The bending strength of a specimen coated with colloidal SiO_2 on the surface was found to have increased by a wider margin [15]. Therefore, further study of the behavior of colloidal SiO_2 for crack-healing still remains to be done.

*Corresponding author:
Tel : +82-51-629-6358
Fax: +82-51-629-6353
E-mail: namkw@pknu.ac.kr

This study also examined the surface morphology in order to ascertain the amount of colloidal SiO_2 needed to influence the bending strength and crack-healing behavior of Si_3N_4 com-posite ceramics, as well as the effects of the surface coating.

Materials and Experimental Methods

A powder composed of 0.2 μm Si_3N_4, 0.27 μm SiC and a sintering additive (33 nm Y_2O_3, commercial anatase TiO_2, and 12% colloidal SiO_2) were used for the experiments. The batch compositions of the specimens are given in Table 1. 0.0 wt.% and 1.3 wt.% of the sintering additive 12% colloidal SiO_2 were used to analyze the influence on the crack-healing behavior. In addition, the crack-healing effects of coating 12% colloidal SiO_2 on a cracked part were also analyzed. When sintered or heat treated, the colloidal SiO_2 forms SiO_2 oxides at temperatures higher than 500 °C. A sintering flow chart of the composite

Table 1. Batch composition of specimens (wt.%)

	Si_3N_4	SiC	Y_2O_3	TiO_2	SiO_2 colloidal	SiO_2 colloidal coating on crack
SS	80	20	8.0	0.0	0.0	Yes
SST-1			5.0	3.0	0.0	No
SST-2			5.0	3.0	0.0	Yes
SSTS			5.0	3.0	1.3	Yes

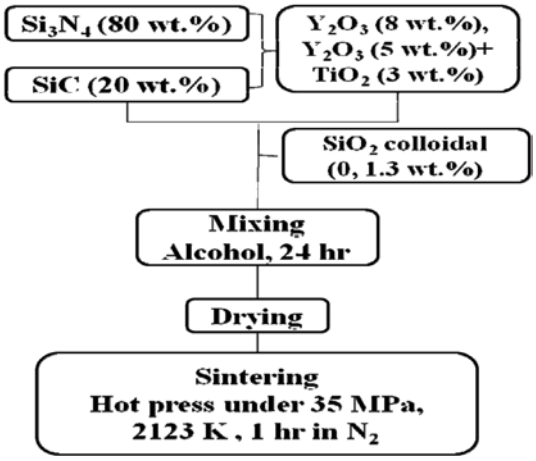

Fig. 1. Sintering flow chart.

ceramics is exhibited in Fig. 1. After having been cut into 3.0 × 4.0 × 22 mm size specimens from the sintered material, polished and then chamfered, all fracture tests were performed on a three-point loading system with a span of 16 mm and a cross head speed of 0.5 mm/minute.

A pre-crack of about 100 μm in length was made at the center of the tensile surface of specimens with a Vickers indenter using a load of 24.5 N. The heat treatment for the optimum crack healing conditions was carried out at an atmospheric level for one hour under temperatures ranging from 773~1,573 K. To analyze the effect of the colloidal SiO_2 on crack healing, heat treatment was conducted after coating the colloidal SiO_2 on the cracked surface under the same conditions. The crack healing phenomena were observed in-situ at an atmospheric level for one hour at temperatures of 1,273 K and 1,573 K. The surface state and surface roughness of the crack healed specimen was also examined using an SPM (scanning probe microscope). A FESEM (Field Emission Scanning Electron Microscope) and EPMA (Electron Probe X-Ray Micro Analyzer) were employed to analyze the composition of the sintering materials.

Inorganic hybrid binder by Sol-Gel process

In general, the hybrid organic-inorganic binder sol uniformly disperses solid particles that are less than 1 μm in size during the liquid phase. The sol is regarded as being stable when there is little interaction between the particles, or when the particles exhibit a form of repulsive force, such as an electrostatic repulsive-force. However, the sol loses its fluidity and becomes a gel when the growth of particles or changes in the charge state result in a strong attractive force occurring between the dispersed particles. There are two known methods of creating an organic-inorganic hybrid binder. One involves the dispersal of the precipitates created by the aggregation of fine particles in the electrolyte, and the other is an increase of the size of molecules or ions into appropriately-sized particles. However, the organic-inorganic hybrid binder sol can also be created through the hydrolysis of metal alkoxide.

Expressing metal alkoxide as $Me(OR)_n$, then the $Me(OH)_n$ produced through the hydrolysis conducted in equation (1) is found to react in the manner seen in equation (2).

$$Me(OR)_n + nH_2O \rightarrow Me(OH)_n + nROH \quad (1)$$

Here, Me indicate metals such as Si, Ti, Al etc; R indicates alkyl groups such as CH_3, C_2H_5 and C_3H_7; and n indicates the relevant metal's oxidation number.

$$Me(OH)_n \rightarrow MeO_{n/2} + n/2\ H_2O \quad (2)$$

$Me(OH)_n$ is then put through chain and condensation reactions following equation (2) to form fine oxidized particles that feature the combination structure -Me-O-Me-O- in the medium. Fig. 2 displays the basic process through which this inorganic hybrid binder sol-gel process is created.

Results and Discussions

Bending strength of crack healed specimen

Fig. 3 exhibits the relationship between crack healing temperature and bending strength based on the type of additive present. ◑ indicates the SS specimen, • indicates the SST-1 specimen, indicates the SST-2 specimen, and indicates the SSTS specimen. The average bending strength of the smooth specimens were 568 MPa (SS), 595 MPa (SST) and 935 MPa (SSTS). The high bending strength of

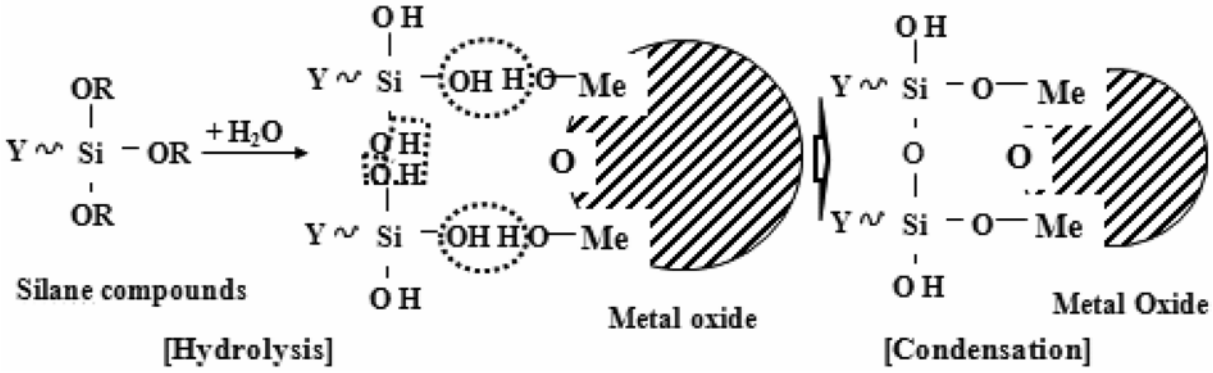

Fig. 2. Principle concept of Sol-Gel process.

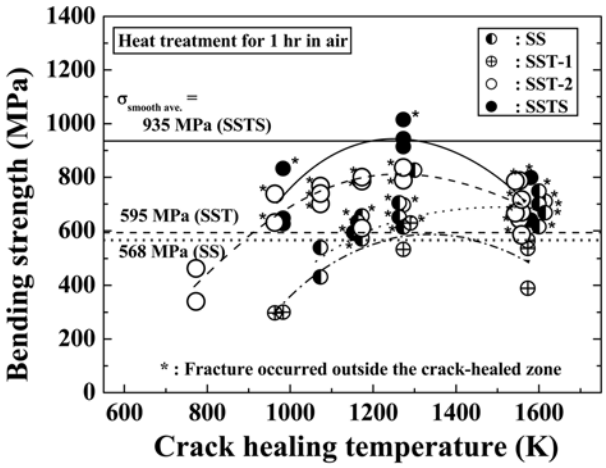

Fig. 3. Relationship of bending strength and crack healing temperature according of the types of specimen.

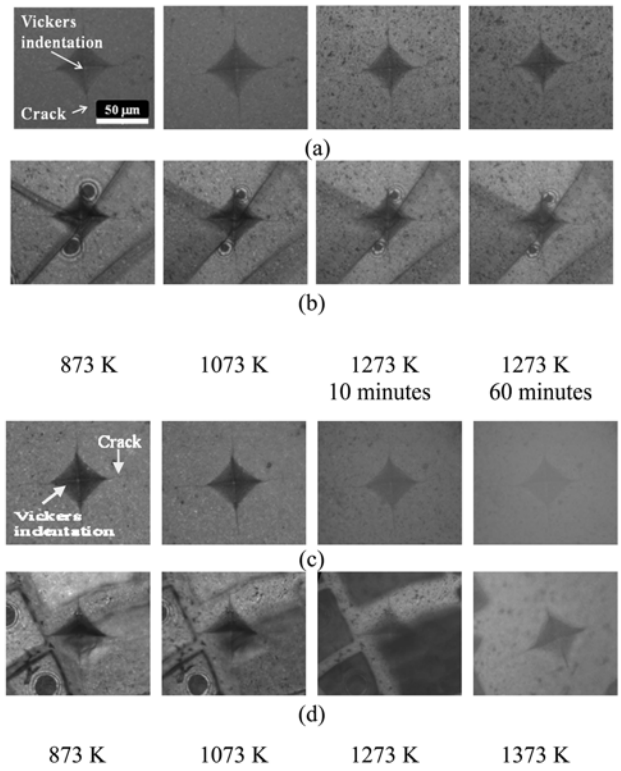

Fig. 4. Crack healing process of in-situ observations using SST specimens; (a) and (b) at 1,273 K, (c) and (d) at 1,573 K; (a) and (c) without a colloidal SiO_2 coating, (b) and (d) with a colloidal SiO_2 coating.

the SSTS specimen can be explained by the fact that as the colloidal SiO_2 was used as the crack-healing agent, the bending strength was significantly increased when the colloidal SiO_2 was added. The SS crack healed specimen coated with colloidal SiO_2 obtained a maximum strength at 1,573 K. The SST-1 crack-healed specimen obtained a maximum strength at 1,273 K. Meanwhile, the SST-2 crack-healed specimen coated with colloidal SiO_2 obtained a maximum strength at 1,273 K. As such, it was revealed that the addition of TiO_2 as the sintering additive decreased the crack-healing temperature by 300 K. It was also revealed that the SSTS specimen with the additive colloidal SiO_2 exhibited a higher bending strength than the SST-2 specimen at 1,273 K.

We also found that the bending strength of crack-healed specimens varied based on whether the colloidal SiO_2 was coated on or not. The SST-1 crack-healed specimen uncoated with the colloidal SiO_2 exhibited a bending strength that was similar to that of the SST smooth specimen. However, the bending strength of the SST-2 crack-healed specimen coated with the colloidal SiO_2 was 140% greater than that of the SST smooth specimen. Furthermore, the bending strength of the SSTS crack-healed specimen coated with the colloidal SiO_2 in which 1.3 wt.% of the additive colloidal SiO_2 was also employed was 160% higher than that of the SST smooth specimen. In Fig. 3, the symbol* indicates fracture occurred outside the crack-healed zone.

In-situ observation of crack healing phenomenon

Fig. 4 shows the state of in-situ crack healing of the SST specimen during one hour at 1,273 K and 1,573 K. (a) and (b) indicate the in-situ at 1,273 K while (c) and (d) indicate the in-situ at 1,573 K. (a) and (c) indicate the specimens without a colloidal SiO_2 coating, while (b) and (d) indicate the specimens with a colloidal SiO_2 coating. The in-situ observations revealed that at a temperature of 1,273 K (a) and (b) exhibited cracks on the surface even after an hour. As a fog emerged when the temperature was over 1,273 K, the in-situ observation of (c) and (d) was difficult to conduct at a temperature of 1,573 K.

In order to analyze the cause of these results, the crack-healed surfaces and surface roughnesses of the specimens observed in-situ were examined using an SPM. The results are shown in Fig. 5. In (a), to which the colloidal SiO_2 was not coated and heat treatment was conducted at 1,273 K, and (b), to which the colloidal SiO_2 was coated and the heat treatment was conducted at 1,273 K, cracks were completely healed. Nevertheless, we can see that the surface of (a) is a little bit rougher than the surface of (b). Meanwhile, (c) and (d), both of which involved heat treatment being conducted at 1,573 K, exhibited a tendency that was similar to (a) and (b), where the heat treatment was carried out at 1,273 K. However, certain cracks are still visible in the cases of (c) and (d) and their surfaces are rougher than was the case with (a) and (b). These differences can be regarded as the causes of the decrease in crack-healing strength. We were thus able to determine the materials in which oxides cause an increase in crack-healing strength using an EPMA analysis [8, 12]. The crack healing reactions of Si_3N_4 composite ceramics are as follows [16]:

$$Si_3N_4 + 3O_2 + SiO_2 \rightarrow 4SiO_2 + 2N_2 \quad (3)$$

$$SiC + SiO_2 + 2O_2 \rightarrow 2SiO_2 + CO_2(CO) \quad (4)$$

$$2SiC + 2Y_2O_3 + 2TiO_2 + SiO_2 + 4O_2 \rightarrow Y_2Si_2O_7 + Y_2Ti_2O_7 + SiO_2 + 2CO_2 \quad (5)$$

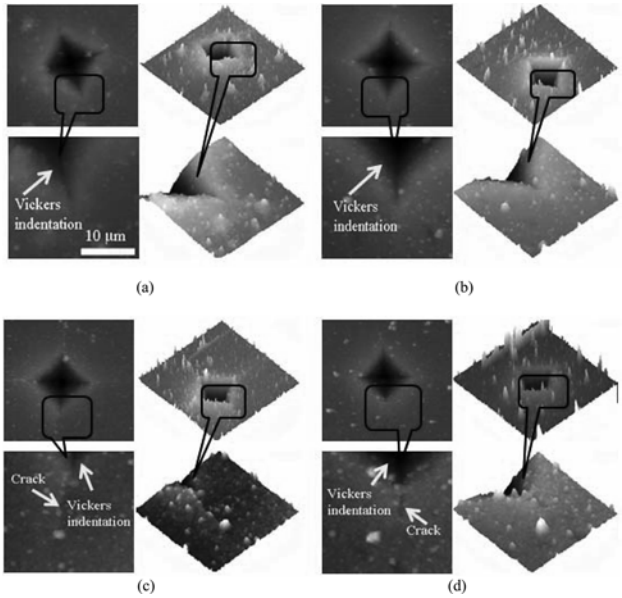

Fig. 5. crack healing appearance and surface roughness by SPM.
(a) without a colloidal SiO_2 coating at 1,273 K
(b) with a colloidal SiO_2 coating at 1,273 K
(c) without a colloidal SiO_2 coating at 1,573 K
(d) with a colloidal SiO_2 coating at 1, 573 K

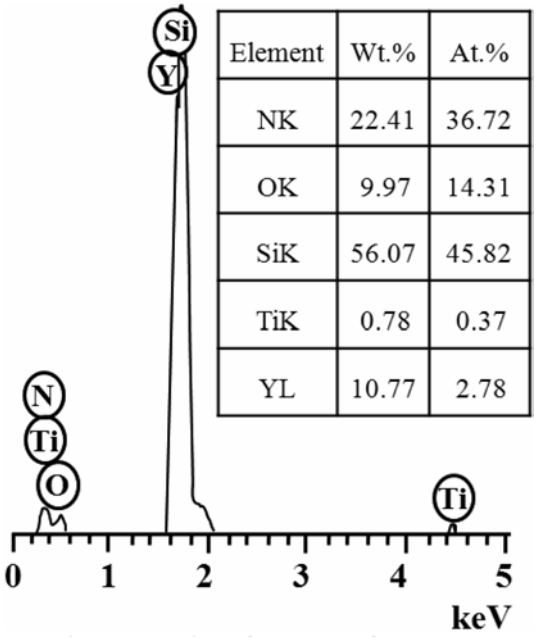

Element	Wt.%	At.%
NK	22.41	36.72
OK	9.97	14.31
SiK	56.07	45.82
TiK	0.78	0.37
YL	10.77	2.78

Fig. 6. Results of FESEM for SST-2.

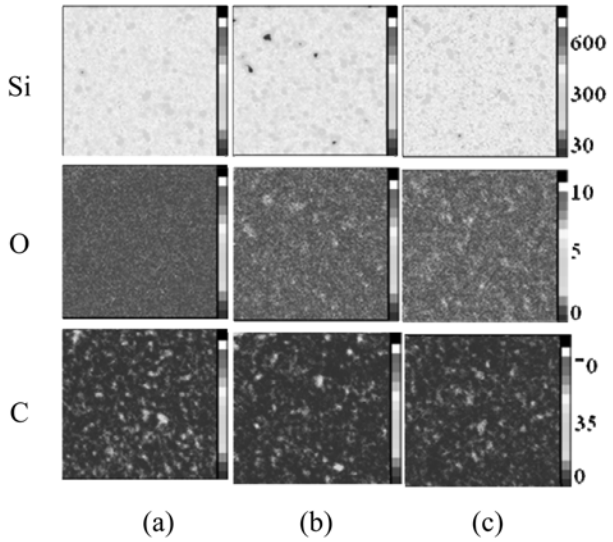

Fig. 7. Elemental mapping by EPMA (SSTS). (a) smooth specimen, (b) crack-healing at 1,273 K, 1 hr in air, (c) crack-healing coated with colloidal SiO_2 at 1,273 K , 1 hr in air.

Here, $Y_2Si_2O_7$ and $Y_2Ti_2O_7$ are crystalline phases. Anatase type TiO_2 becomes a rutile-type crystalline phase at higher than 500 ºC. The SiO_2 has two phases; a glassy and a crystalline phase. The amount of crystallized SiO_2 was dependent on the crack-healing temperature. Therefore, it can be concluded that ceramics containing Si recovered their bending strength by means of glassy phase SiO_2. And, based on the above facts, that the cracks in Fig. 5(c) and (d), which were crack healed at high temperatures, were caused by the vaporization of glassy SiO_2[8].

The oxides which were made by the heat treatment on the surface of the specimen were analyzed using an FESEM. Fig. 6 shows the results of the SST-2 specimen heat treated for an hour at an atmospheric level at 1,273 K. The elements of Ti, Si, Y and O were detected from the surface of the SST-2 specimen. The formation of the crystalline phases of $Y_2Si_2O_7$, $Y_2Ti_2O_7$ and SiO_2 contributes to improving the bending strength.

In order to analyze the basic crack-healing materials, an EPMA was used to develop images of materials such as Si, C and O that had formed on the surface of specimens. Fig. 7 shows the result of the SSTS specimen synthesized with 1.3 wt.% of the additive colloidal SiO_2. In this figure, a large amount of Si and O were detected in (a), (b) and (c). Moreover, while (c), which was coated with the colloidal SiO_2, exhibited even higher amounts of Si and O, it featured slightly lower levels of C. This fact clearly indicates that the colloidal SiO_2 does in fact have an effect on crack healing.

Conclusions

Si_3N_4 composite ceramics were sintered and subjected to three-point bending tests. This study examined the surface morphology as part of a wider effort to analyze the influence of the bending strength and crack-healing behavior by additive colloidal SiO_2 and colloidal SiO_2 coating. The main results are as follows;

1) The sintering additive TiO_2 decreased the crack-healing temperature by 300 K. Moreover, the bending strength of the specimens with the additive colloidal SiO_2 was found to be higher. Furthermore, the bending strength of the specimen coated with the colloidal SiO_2 was revealed to be higher than that of the specimen without a colloidal SiO_2 coating.

2) In-situ observation revealed that a fog emerged on

a surface of the crack-healed specimen at 1,537 K. Moreover, an SPM revealed that while both the crack-healed specimen coated with the colloidal SiO_2 and the one without the colloidal SiO_2 coating exhibited complete crack healing at 1,273 K, cracks remained in the case of both crack-healed specimens at 1,573 K. These were the result of the vaporizing of the SiO_2 at high temperatures.

3) The crack healing materials of Si_3N_4 composite ceramics created by crack-healing reactions include the crystal phases of $Y_2Si_2O_7$, $Y_2Ti_2O_7$ and SiO_2.

4) Significant amounts of Si and O and slight amounts of C were detected through an EPMA-based analysis of crack-healed material. Large amounts of Si and O were detected on the SSTS specimens. Specimens coated with the colloidal SiO_2 exhibited higher amounts of Si and O but somewhat decreased levels of C. The above test results demonstrated that the colloidal SiO_2 does in fact have an effect on crack healing.

References

1. J.J. Petrovic and L.A. Jacobson, J. Am. Ceram. Soc., 59 (1976) 34-37.
2. T.K. Gupta, J. Am. Ceram. Soc., 59 (1976) 259-262.
3. S.R. Choi and V. Tikare, Scr. Metall. Mater., 26 (1992) 1263-1268.
4. J.E. Moffatt, W.J. Plumbridge and R. Hermann, Br. Ceram. Trans., 95 (1996) 23-29.
5. M.C. Chu, S. Sato, Y. Kobayashi and K. Ando, Fatigue Fract. Eng. Mater. Struct., 18 (1995) 1019-1029.
6. M.C. Chu, S. Sato, Y. Kobayashi and K. Ando, Jpn. Soc. Mech. Eng., 60 (1994) 2829-2834.
7. Y.Z. Zhang, L. Edwards and W.J. Plumbridge, J. Am. Ceram. Soc., 81 (1998) 34-37.
8. K. Ando, T. Ikeda, S. Sato, F. Yao and Y. Kobayashi, Fatigue Fract. Eng. Mater. Struct., 21 (1998) 119-122.
9. K. Ando, Y. Shirai, M. Nakatani, Y. Kobayashi and S. Sato, J. Eur. Ceram. Soc., 22 (2002) 121-128.
10. K. Ando, K. Houjyou, M. C. Chu, S. Takeshita, K. Takahashi, S. Sakamoto and S. Sato, J. Eur. Ceram. Soc., 22 (2002) 1339-1346.
11. S.K. Lee, W. Ishida, S.Y. Lee, K.W. Nam and K. Ando, J. Eur. Ceram. Soc., 25 (2005) 569-576.
12. K.W. Nam, H.S. Kim, C.S. Son, S.K. Kim and S.H. Ahn, Transactions of the KSME(A), 31 (2007) 1108-1114.
13. H.S. Kim, M.K. Kim, J.W. Kim, S.H. Ahn and K.W. Nam, Transactions of the KSME(A), 31 (2007) 425-431.
14. K.W. Nam, M.K. Kim, H.S. Kim, J.W. Kim and S.H. Ahn, International Journal of Modern Physics B, 20 (2006) 4279-4284.
15. K.W. Nam, M.K. Kim, S.W. Park, S.H. Ahn and J.S. Kim, Materials Science and Engineering(A), 471 (2007) 102-105.
16. M.K. Kim, S.B. Kang, S.H. Ahn and K.W. Nam, Solid State Phenomena, 124-126 (2007) 719-722.